Published in final edited form as:

J Immunol. 2017 January 01; 198(1): 147–155. doi:10.4049/jimmunol.1601218.

Sensitivity to restimulation-induced cell death is linked to glycolytic metabolism in human T cells

Sasha E. Larsen[*], **Abegail Bilenkin**[*], **Tatiana N. Tarasenko**[†], **Swadhinya Arjunaraja**[*], **Jeffrey R. Stinson**[*], **Peter J. McGuire**[†], and **Andrew L. Snow**[*,1]

[*]Department of Pharmacology & Molecular Therapeutics, Uniformed Services University of the Health Sciences, Bethesda, MD

[†]Metabolism, Infection and Immunity Unit, NHGRI, National Institutes of Health, Bethesda, MD

Abstract

Restimulation-induced cell death (RICD) regulates immune responses by restraining effector T cell expansion and limiting nonspecific damage to the host. RICD is triggered by re-engagement of the T cell receptor (TCR) on a cycling effector T cell, resulting in apoptosis. It remains unclear how RICD sensitivity is calibrated in T cells derived from different individuals or subsets. Here we show that aerobic glycolysis strongly correlates with RICD sensitivity in human $CD8^+$ effector T cells. Reducing glycolytic activity or glucose availability rendered effector T cells significantly less sensitive to RICD. We found that active glycolysis specifically facilitates the induction of pro-apoptotic Fas ligand upon TCR restimulation, accounting for enhanced RICD sensitivity in highly glycolytic T cells. Collectively, these data indicate that RICD susceptibility is linked to metabolic reprogramming, and that switching back to metabolic quiescence may help shield T cells from RICD as they transition into the memory pool.

Introduction

Dynamic changes in cellular metabolism are vital during the course of an effective $CD8^+$ T cell response. Like most somatic cells, naïve and memory T cells operate in a generally quiescent metabolic state and utilize mitochondrial oxidative phosphorylation (OXPHOS) for ATP generation (1). Following T cell receptor (TCR) stimulation, however, responding T cells rapidly switch to using glycolysis even in the presence of oxygen (Warburg effect) (2-4). Activated T cells proliferate and acquire potent effector functions (e.g. IFN-γ production), which have been linked to glycolytic metabolism (2, 4-8). Recent reports demonstrate that changes in cellular metabolism over the course of a T cell response profoundly influence cell survival and differentiation, including the generation of memory (2, 4, 8-13). Interestingly, it is precisely during this window of expansion and aerobic

Address correspondence to: Andrew L. Snow, Ph.D., Tel: 301-295-3267, Fax: 301-295-3220, andrew.snow@usuhs.edu.

[1]This work was supported by grants from the National Institutes of Health (R01GM105821 to A.L.S.) and USUHS (to S.E.L. and A.L.S.).

Disclosures

The authors have no financial conflicts of interest.

glycolysis that effector T cells become sensitive to activation-/restimulation-induced cell death (AICD/RICD).

Restimulation induced cell death (RICD) is a critical apoptotic program that ultimately sets an upper limit for effector T cell expansion during an infection. RICD sensitivity is dependent on prior activation, cell cycle induction via interleukin-2 (IL-2), and a subsequent, strong restimulation signal propagated through the TCR, which induces apoptosis in a subset of effectors (14-16). Unlike effector T cells, naïve and resting memory T cells are relatively resistant to RICD. By constraining effector T cell numbers during the antigen-induced expansion phase, this self-regulatory death pathway helps to maintain immune homeostasis by precluding excessive, non-specific immunopathological damage to the host. Indeed, our lab previously demonstrated that a defect in RICD contributes to excessive T cell accumulation and lethal damage to host tissues, as noted in patients with X-linked lymphoproliferative disorder (17, 18).

Although RICD was first described over 25 years ago (16, 19-21), the molecular components that convert TCR signaling from pro-proliferative in naïve cells to pro-apoptotic in restimulated, activated T cells have yet to be fully defined. Additionally, it remains unclear why RICD sensitivity varies for T cells from different normal human donors, and why only a proportion of expanded effector T cells are rendered competent to die after TCR restimulation. Although robust glycolytic metabolism overlaps closely with the window of RICD susceptibility in effector T cells, it is not known whether metabolic reprogramming influences RICD directly. We hypothesized that glycolytic metabolism promotes the sensitization of effector T cells to RICD. Here we show for the first time that active glycolysis enhances RICD in effector $CD8^+$ T cells, specifically by enabling robust induction of Fas ligand (FASL) after TCR restimulation. Our findings suggest that restricting glucose availability and/or reducing glycolysis may prolong the survival of activated T cells by protecting them from RICD.

Materials and Methods

Isolation, activation and culture of primary human $CD8^+$ T cells

Blood from anonymous healthy donors (buffy coats) was generously provided by Dr. Michael Lenardo and the National Institutes of Health Blood Bank. PBMC were isolated using Ficoll density gradient centrifugation, and $CD8^+$ T cells were purified from PBMC using the EasySep Human $CD8^+$ T cell enrichment kit (Stem Cell Technologies). T cells were activated 1:1 with beads coated with anti-CD3/CD2/CD28 antibodies (Human T cell Activation/Expansion Kit, Miltenyi) in glucose-free RPMI 1640 (Life Technologies) + 10% dialyzed fetal calf serum (FCS) (Life Technologies) + 1mM sodium pyruvate (Cellgro) + 1% penicillin/streptomycin (Lonza) and either 10 mM D-galactose or D-glucose (Sigma) for 3 days. Activated T cells were washed in PBS and subsequently cultured in glucose- or galactose-containing media with 100 U/mL rIL-2 (PeproTech) at 1×10^6 cells/mL for ≥13 days, changing media every 3 days. In some experiments, cells on days 9-12 were washed 2x in PBS and swapped into media containing the opposite sugar as described in the Figure Legends. For conditioned media experiments, Glc and Gal T cell cultures were spun down on day 14 of culture in IL-2 and cells were resuspended in the opposite conditioned culture

media with additional IL-2. These cells were incubated for 30 minutes and then assayed for RICD as described below. Additionally, cells grown in galactose were washed 2x in PBS and resuspended in media supplemented with 10-fold titrations of glucose prior to RICD assays as described.

Apoptosis assays, transfections and flow cytometry

RICD assays were performed as previously described (22). Briefly, activated T cells (days 13-15) were treated in triplicate with anti-CD3ε mAb OKT3 (5–500 ng/ml; Biogems), and plated at 7.5×10^5 cells/mL in 96-well round bottom plates. For some assays, cells were pretreated for 30 min with 2 μM 2-deoxy-glucose (2-DG), 2.7 μM rapamycin, 1 μM oligomycin A, 5 μM rotenone, 10 ng/mL rIFNγ, 5 μg/mL concanamycin A, 20 mM D-glucose (Sigma-Aldrich) or 1 μg/mL anti-FAS antagonistic antibody SM1/23 (Enzo) versus DMSO or ddH_20 solvent control. At 24h after TCR restimulation, cells were stained with 5 μg/mL propidium iodide (Sigma-Aldrich) and collected for constant time on an Accuri C6 flow cytometer (BD Biosciences). Cell death was quantified as percentage cell loss = (1 – [number of viable cells (treated) / number of viable cells (untreated)]) × 100. For some assays, T cells were stained with Annexin V-FITC (BioLegend) 4 hours after restimulation. Surface expression of FAS (CD95) and CD3 were assessed using anti-CD95-APC and anti-CD3-PE antibodies respectively (BioLegend). Surface expression of CD107a (LAMP1) was measured ± 4 hours of anti-CD3 restimulation using anti-CD107a-APC (BioLegend). Intracellular flow cytometry for phospho-S6 at baseline and after 4 hours of restimulation ± 2-DG pretreatment was measured using anti-pS6-FITC (Cell Signaling) with Cytofix Fixation Buffer and Phosflow Perm Buffer III reagents according to product protocol (BD Biosciences). DNA content was used to evaluate cell cycle status ± 4 hours of anti-CD3 restimulation using methanol fixation and staining with PI and RNAse A (Sigma). Cell cycle status was also assessed using the Click-iT EdU (Thermo Fisher) assay by flow cytometry, according to product protocol. Transfections of Glc and Gal T cells were performed with 5 μg of either pEGFP-C2 or pEGFP-C2-FASL-3'UTR plasmids, a generous gift from the Gallouzi lab (23), using the Amaxa P3 Primary Cell 4D-Nucleofactor X Kit L (Lonza) according to the manufacturer's protocol. GFP expression was analyzed 6 hours post-transfection by flow cytometry. All flow cytometric assays were performed on an Accuri C6 flow cytometer (BD Biosciences).

OCR & ECAR measurement

Oxygen consumption and extracellular acidification rates (OCR and ECAR) were measured using a Seahorse XF24 analyzer (Seahorse Bioscience). Primary human effector T cells derived in glucose-containing media (as described above) were attached with Cell-Tak tissue adhesive (Corning) to 24-well Seahorse XF-24 assay plate at approximately 500,000 cells/well in Seahorse BASE media with additives. Cells were incubated at 37°C in a non-CO2 incubator for 45 minutes. All media was adjusted to pH 7.4 on the day of assay. Mitochondrial and glycolysis stress tests were performed according to the manufacturer's protocol. OCR (an indicator of oxidative phosphorylation) and ECAR (an indicator of glycolysis) were automatically calculated and recorded by the Seahorse XF-24 software.

Western blotting

Activated $CD8^+$ T cells (1×10^6 per time point) were restimulated with 500 ng/ml OKT3 (0–4hr), washed in cold PBS, and lysed in 1% Nonidet P-40 (NP-40) lysis buffer (50 mM Tris [pH 7.4], 150 mM NaCl, 0.5 mM EDTA, 1% NP-40, 0.5% sodium deoxycholate, 1 mM Na_3VO_4, 1 mM NaF) containing complete protease inhibitors (Roche) for 30 min on ice. Cleared lysates were boiled in 2x reducing sample buffer, and resolved on Any kD SDS-PAGE gels (Bio-Rad). Proteins were transferred to nitrocellulose on a Trans-Blot Turbo system (Bio-Rad), blocked in 2% Tropix I-Block (Applied Biosystems) in TBS/0.1% Tween, and probed with the following Abs: anti-FASL (Ab3; EMD Millipore); anti-BID; anti-cleaved caspase 8 (Cell Signaling Technologies); anti-BIM (Enzo); anti-cleaved caspase 9, anti-cleaved caspase 3, anti-NUR77 (Biolegend); anti-geminin; anti-Cdt1 (Santa Cruz Biotechnology) and anti–β-actin (Sigma-Aldrich). Bound Abs were detected using HRP-conjugated secondary Abs (Southern Biotech, eBioscience) and ECL (Thermo Scientific).

ELISA

Detection of soluble/cleaved FASL in cell supernatants from T cells −/+ anti-CD3 restimulation (−/+ inhibitor pre-treatment as described above) was performed using the Quantikine Human Fas Ligand/TNFSF6 Immunoassay Kit (R&D Systems). L-lactate levels were measured in cell supernatants using a Glycolysis Cell-based Assay kit (Cayman Chemical). IFN-γ secretion was measured in cell supernatants from T cells −/+ anti-CD3 restimulation using the Ready SET Go Human ELISA IFN-γ kit (eBioscience). ELISA plates were read using a Synergy H1 Hybrid Reader (BioTek); concentrations of sFASL (pg/ml), L-lactate (μM) or IFN-γ (pg/ml) were calculated using Gen5 data analysis software (BioTek).

Quantitative PCR

RNA was isolated from Glc or Gal T cells from 2 donors at baseline or after 4 hours of OKT3 restimulation ± 2DG pretreatment using QIAshredder and RNeasy mini plus columns (Qiagen). cDNA was prepared from 300 ng RNA using the MultiScribe Reverse Transcriptase Kit (ThermoFisher Scientific). Maxima SYBR Green/ROX qPCR Master Mix (ThermoFisher Scientific) was used for subsequent PCR with specific primers against FASL (for: CTTCCACCTACAGAAGGAGC, rev: CCAGAAAGCAGGACAATTCC) and RPL13 (for: GAATGGCATGGTCTTGAAGCC, rev: GGGAATGTGCTGTTTCCATGG) as a reference control, analyzed on a StepOnePlus Real-Time PCR System (Applied Biosystems).

Statistics

In vitro cell death assays were evaluated using two-way ANOVA (α=0.05) with Sidak correction for multiple comparisons or students T-Test where appropriate. L-lactate, maximum ECAR, OCR, % cell loss and sFASL values were correlated using Pearson's comparison analysis and graphs were generated using linear regression. All statistical analyses were performed using GraphPad PRISM software. Error bars are defined in the figure legends as ± SEM or ± SD where appropriate. Asterisks denote statistical significance and p-values are reported in figure legends.

Results

To investigate whether donor-dependent variability in RICD sensitivity is associated with glycolytic metabolism, we first measured RICD and L-lactate production in $CD8^+$ effector T cells derived from three human donors after restimulation with the agonistic anti-CD3 antibody OKT3. Donor T cells that displayed higher RICD sensitivity also produced more L-lactate, a secreted product of glycolysis, after 4 hours of restimulation (Fig. 1A,B). Indeed, when data collected from 12 donors were subjected to linear regression analysis, we found a significant correlation existed between RICD sensitivity and L-lactate measured in the supernatant (Fig. 1C, R=0.8772). Consistently, the maximum extracellular acidification rate (ECAR) achieved after TCR restimulation also demonstrated significant correlation with RICD sensitivity in 6 donors with variable sensitivity (Fig. 1D-F, R=0.9142). In contrast, oxygen consumption rate (OCR) as a measure of oxidative phosphorylation (OXPHOS) did not significantly correlate with RICD sensitivity in the same 6 donors tested (Fig. S1A,B). Moreover, effector T cells treated with oligomycin A (mitochondrial ATP synthase inhibitor) or rotenone (electron transport complex I inhibitor) showed only a slight, non-significant increase in RICD sensitivity (Fig. S1C,D). These data suggest that RICD sensitivity directly correlates with glycolytic activity, but not OXPHOS, in human $CD8^+$ T cells.

To establish a causal link between glycolytic metabolism and RICD, we next expanded effector T cells from single donors in glucose-versus galactose-containing culture medium. Substituting galactose for glucose severely restricts glycolysis and forces T cells to predominantly use OXPHOS (24). Interestingly, donor T cells cultured in galactose (Gal) culture media were significantly less sensitive to RICD compared to T cells cultured in glucose (Glc) containing media (Fig 1G). This difference could not be explained by a broader defect in programmed cell death, as both Glc- and Gal-cultured T cells were equally sensitive to direct FAS ligation (Fig. 1H). Glc and Gal-cultured T cells also displayed equivalent cell surface expression of T cell receptor (CD3) and FAS (CD95) (Fig. 1I). These data imply that RICD susceptibility is specifically influenced by metabolic status in effector T cells.

To explore the link between glycolysis and RICD, we conducted further apoptosis assays comparing Glc versus Gal T cells in the presence of the competitive glucose analog 2-deoxyglucose (2-DG) (7). Brief pre-treatment with 2-DG substantially reduced the number of 4 hour restimulated Glc T cells staining positive with Annexin V, an early marker of apoptosis commitment, and significantly reduced RICD sensitivity at 24 hours (Fig. 2A,B). Indeed, Glc T cells treated with 2-DG showed a dramatic reduction in L-lactate production after 4 hours of restimulation, confirming decreased glycolysis (Fig. 2C). Although Gal T cells primarily utilize OXPHOS, galactose can be used for glycolysis at much lower efficiency than glucose (25). Hence 2-DG also reduced RICD sensitivity in Gal T cells (Fig. 2B), associated with a detectable decrease in lactate production in most donors tested (Fig. 2C). These results indicate that acute inhibition of glycolysis renders T cells less sensitive to RICD.

We next asked whether RICD sensitivity of effector T cells relying primarily on glycolysis versus OXPHOS could be altered by prolonged or acute changes in glucose availability. Interestingly, we could generate a step-wise reduction in Glc T cell RICD sensitivity by swapping cells into galactose-containing media for 1-5 days of culture prior to restimulation (Fig. 2D). Conversely, supplementing normal culture media with additional glucose further increased RICD of Glc T cells slightly, reaching maximum sensitivity at 20 mM (data not shown). Since Gal T cells preferentially use pyruvate for the TCA cycle, they lack excess pyruvate for subsequent conversion to secreted L-lactate. We therefore asked whether extracellular L-lactate was sensitizing Glc T cells to RICD by swapping Glc T cells into galactose-conditioned culture media (low L-lactate) and Gal T cells into glucose-conditioned culture (high L-lactate). We saw no increase in Gal RICD sensitivity in the glucose-conditioned media compared to Gal T cells in galactose-containing media (Fig. 2E), suggesting that (a) excess L-lactate and/or other secreted factors did not provide a sensitizing feedback signal to Glc T cells, and (b) little to no glucose remained in the glucose-conditioned media. Conversely, Gal T cells swapped into fresh10 mM glucose-containing media for just 30 minutes were notably more sensitive to RICD (Fig. 2F). This enhanced RICD sensitivity was titratable and decreased with serial 10-fold dilutions of glucose in the media (Fig. 2F). The addition of 2-DG helped accentuate these differences, presumably by impeding hexokinase activity and restricting the entry of freshly added glucose into the glycolytic cycle. Collectively, these data imply that acute glucose availability helps set the threshold for RICD sensitivity in $CD8^+$ effector T cells.

To understand how glycolytic metabolism drives RICD sensitivity, we examined several requirements known to render effector T cells competent to die through this pathway. Because only effector T cells that are actively cycling are sensitive to RICD (15, 26, 27), we next asked whether cell cycle progression was specifically enhanced in Glc T cells before or after TCR restimulation, relative to Gal T cells. Using PI cell cycle analysis, we found an equal percentage of cells actively dividing (S + G2/M phases) at baseline in both Glc and Gal T cells (Fig. 3A). After 4 hours of restimulation, we measured a lower percentage of Glc T cells in cycle compared to Gal T cells, which was rescued by pre-treatment with 2-DG (Fig. 3A). Glc T cell cultures displayed a concomitant increase in the proportion of sub-G1/apoptotic cells, consistent with RICD induction (Fig. 3A). Immunoblotting also showed no marked changes in the expression of key cell cycle checkpoint proteins Cdc10-dependent transcript 1 (Cdt-1) and geminin at baseline, after 4 hours restimulation, or with 2-DG treatment between Glc and Gal T effector cells (28) (Fig. S2). We further corroborated these findings by examining cell proliferation before and after 4 hours of restimulation. Glc and Gal T cells demonstrated equivalent EdU incorporation in all conditions tested (Fig. 3B). These data suggest that Glc T cells are not more sensitive to RICD simply because a greater proportion of cells are proliferating or induced into cell cycle upon TCR restimulation.

IFN-γ has also been implicated in potentiating RICD sensitivity (29). Previous studies demonstrated that T cells cultured in Gal media proliferate but cannot mount sufficient effector functions, including IFN-γ secretion (6, 7, 24). We confirmed a similar defect in IFN-γ secretion by Gal T cells (Fig 3C). However, the addition of exogenous IFN-γ did not boost RICD sensitivity in Gal T cells to levels measured in Glc T cells (Fig. 3D). Interestingly, Gal T cells actually demonstrated greater CD107a (LAMP1) staining by flow

cytometry at baseline and after 4 hours of restimulation than Glc T cells (Fig 3E). Moreover, inhibition of lytic granule maturation with concanamycin A (CMA) (30) treatment did not preferentially decrease Glc T cell sensitivity (Fig. 3F). These data suggest that diminished RICD sensitivity of Gal T cells is not explained by deficiencies in IFN-γ production or perforin-mediated cytotoxicity.

We subsequently investigated whether RICD sensitivity is influenced by mammalian target of rapamycin complex 1 (mTORC1) and c-Myc, critical signaling nodes activated during glycolysis that promote anabolic metabolism (31). Treatment with rapamycin reduced RICD of Glc and Gal T cells slightly, but did not eliminate the death sensitivity difference between these subsets (Fig 4A). As expected, Glc T cells displayed higher phosphorylated ribosomal protein S6 (pS6) staining, a surrogate for mTORC1 activity, at baseline and after 4 hours of restimulation compared to Gal T cells. Whereas pre-treatment with 2-DG partially reduced the pS6 signal, rapamycin reduced pS6 activity following restimulation in both Glc and Gal T cells to levels below baseline, indicating potent inhibition of mTORC1 activity. We also observed equivalent expression of c-Myc in Glc and Gal T cells ± restimulation, with no change in RICD observed after pretreatment with c-Myc inhibitor JQ1 (data not shown) (32). Together these data suggest that the difference in RICD sensitivity noted between Glc and Gal T cells is largely independent of mTORC1 activity and c-Myc signaling.

To determine the mechanism by which glycolysis promotes the execution of RICD, we generated cell lysates from Glc versus Gal T cells pre- and post TCR restimulation to compare expression of critical pro-apoptotic proteins. As reported previously, immunoblotting revealed a robust *de novo* induction of full-length FASL in Glc T cells, much of which is rapidly cleaved at the plasma membrane to generate a prominent N-terminal fragment (Fig 5A) (18). Strikingly, full-length FASL expression was markedly reduced in restimulated Gal T cells after 4 hours of restimulation (Fig. 5A, top panel). Consistent with a reduction in RICD sensitivity, full-length FASL induction in Glc T cells was almost completely blocked with 2-DG treatment (Fig. 5A). We also noted a concomitant reduction in cleaved BID, active caspase-8, caspase-9 and caspase-3 in Gal T cells, or in Glc T cells with 2-DG treatment (Fig. 5A). In contrast, the induction of other pro-apoptotic proteins important for RICD of $CD8^+$ T cells, including BIM and NUR77, was normal for all culture conditions tested (Fig. 5A) (17, 18). An ELISA confirmed the differential induction of FASL in Glc vs. Gal T cells after restimulation, with more release of soluble FASL (sFASL) in Glc versus Gal T cell supernatants from each donor tested (Fig 5B). Although the “sFASL” detected here may include both soluble, cleaved FASL (relatively inactive) and exosomal FASL (highly active), its detection in the supernatant provides another reliable readout of FASL protein induction, as we have shown previously (18). Consistent with immunoblotting results, TCR-triggered FASL release was substantially reduced with 2-DG pre-treatment (Fig. 5B), but not rapamycin (data not shown).

We next used qPCR to examine transcriptional control of FASL induction in Glc and Gal T cells. Glc T cells expressed significantly more FASL mRNA than Gal T cells at baseline and after restimulation ± 2-DG treatment (Fig. 5C). However, FASL transcription was still robustly induced in Gal T cells after restimulation (Fig. 5C), despite a profound decrease in FASL protein (Fig. 5A). Similarly, 2-DG treatment substantially decreased FASL protein

expression (Fig. 5A) without affecting mRNA levels post-restimulation (Fig. 5C). These data imply that a post-transcriptional mechanism governs the decrease in FASL protein expression observed with restriction of glycolysis in T cells. We confirmed this using a GFP reporter construct linked to the 3' untranslated region (UTR) of FASL mRNA, which is known to regulate FASL protein translation (23). Indeed, the FASL 3'UTR reduced GFP expression significantly more in Gal T cells (Fig. 5D). Additionally, treatment of transfected Glc T cells with 2-DG also reduced FASL 3'UTR-GFP reporter expression (average MFI decrease = 42.3± 5.8%; data not shown). Together these results imply that translation of FASL mRNA in T cells is suppressed under conditions of limited glycolysis.

Importantly, linear regression analysis of Glc T cells from 9 separate donors revealed a strong positive correlation between L-lactate and sFASL protein concentrations in cell supernatants (Fig. 5E, R=0.8033), suggesting a direct association between glycolysis and TCR-induced FASL upregulation in $CD8^+$ effector T cells. To test whether differences in FASL protein induction specifically explained relative RICD sensitivity in Glc vs. Gal T cells, we blocked the death receptor FAS during TCR restimulation. Pretreatment with the antagonistic FAS blocking antibody SM1/23 reduced RICD sensitivity of Glc T cells to a much greater extent than Gal T cells (Fig. 5F). More importantly, FAS blockade completely abolished any difference in RICD sensitivity between Glc and Gal T cells (Fig. 5F). These data suggest that glycolytic metabolism specifically promotes RICD sensitivity in effector $CD8^+$ T cells by permitting robust FASL induction and FAS-mediated apoptosis.

Discussion

This study highlights glycolytic metabolism as a novel requirement for licensing the FASL-dependent component of RICD sensitivity in effector $CD8^+$ T cells. Interestingly, we detected no substantial differences in other known requirements for RICD between Glc and Gal T cells, including TCR expression and IL-2-dependent cell cycling. For proliferating T cells, glycolysis is not only employed for macromolecule synthesis, but is also critical for acquiring full effector functions (3, 6, 24, 25). However, our results suggest differences in IFN-γ or cytolytic granule release cannot account for differential RICD between Glc and Gal T cells. We also noted comparable upregulation of TCR-induced pro-apoptotic molecules BIM and NUR77 following restimulation of Glc versus Gal T cells ± 2-DG treatment. Unlike SAP-deficient T cells, these data imply that decreased RICD is not caused by a global attenuation of downstream TCR signal strength when glycolysis is restricted. Moreover, TCR-induced *de novo* translation of these proteins is still intact under these conditions, explaining why mTORC1 inhibition had a small, comparable effect on RICD of Glc and Gal T cells.

Our data demonstrate that glucose availability and glycolytic activity enhances RICD specifically through the induction of FASL after TCR restimulation. FASL is one of several pro-apoptotic proteins that contribute to RICD of effector T cells (18, 33). Previous work showed that FASL is a TCR-responsive transcriptional target of c-Myc, a crucial driver of glycolytic reprogramming in T cells (31, 34). However, we observed no differences in c-Myc expression for Gal and Glc T cells, and no effect on RICD upon treatment with the c-Myc inhibitor JQ-1 (data not shown). Instead, our data suggest glycolysis enables FASL

expression by releasing FASL mRNA from post-transcriptional repression. Glyceraldehyde 3-phosphate dehydrogenase (GAPDH), which normally catalyzes the sixth step of glycolysis, can bind 3'UTR sequences of cytokine mRNAs (e.g. IFN-γ) to limit their translation, especially when glycolysis is limited (24). However, partial knockdown of GAPDH (75%) failed to rescue FASL expression and boost RICD in Gal T cells (data not shown). It will be of interest to survey other glycolytic intermediates and enzymes for potential "moonlighting" activities in the control of FASL expression (35).

Linking RICD sensitivity to glycolysis provides an elegant control mechanism for maintaining immune homeostasis by precluding the excessive expansion of terminally differentiated, highly glycolytic effector T cells. It will be important to determine whether certain effector T cells that modulate glycolysis and switch to OXPHOS, fatty acid oxidation (FAO), and/or autophagy can preferentially enter the memory pool in part by escaping RICD (5, 31, 36). Recently identified effector T cell subsets such as short-lived effectors (SLEC) and memory precursor (MPEC) T cells differ in their survival and potential for memory formation (37, 38), which may be influenced by a divergence in glycolysis-dependent RICD sensitivity. For example, exposure to cytokines like IL-15 might protect selected effectors from RICD by facilitating a switch from aerobic glycolysis to OXPHOS (4, 38-40).

In linking glycolysis with susceptibility to a specific self-regulatory apoptosis program, our study complements many recent reports tying T cell survival and memory generation to catabolic metabolism (5, 31, 36). We posit that pharmacological interventions that promote memory T cell formation via metabolic reprogramming may work in part by allowing greater numbers of T cells to escape RICD (12, 41). Therefore, agents that alter metabolic programming in T cells may prove useful in regulating the magnitude of any given T cell response specifically by tuning RICD sensitivity, an emerging therapeutic concept for correcting dysregulated immune homeostasis (17).

Supplementary Material

Refer to Web version on PubMed Central for supplementary material.

Acknowledgements

We thank the lab of Dr. Chou-Zen Giam for advice on interrogating cell cycle proteins, Dr. Michael Lenardo and the NIH Blood Bank for providing access to anonymous blood donations, Dr. Barrington Burnett's lab for assistance with qPCR, Dr. Cara Olsen for statistics evaluation, Dr. Imed Gallouzi's lab for GFP reporter plasmids, and Drs. Edward Mitre, Brian Schaefer, Joseph Mattapallil and Pamela Schwartzberg for helpful discussions.

References

1. van der Windt GJ, O'Sullivan D, Everts B, Huang SC, Buck MD, Curtis JD, Chang C-HH, Smith AM, Ai T, Faubert B, Jones RG, Pearce EJ, Pearce EL. CD8 memory T cells have a bioenergetic advantage that underlies their rapid recall ability. Proc. Natl. Acad. Sci. U.S.A. 2013; 110:14336–14341. [PubMed: 23940348]
2. Pearce EL, Poffenberger MC, Chang CH, Jones RG. Fueling immunity: insights into metabolism and lymphocyte function. Science. 2013; 11:12424541–12424552.
3. Lunt SY, Vander Heiden MG. Aerobic glycolysis: meeting the metabolic requirements of cell proliferation. Annu. Rev. Cell Dev. Biol. 2011; 27:441–464. [PubMed: 21985671]

4. Gerriets VA, Rathmell JC. Metabolic pathways in T cell fate and function. Trends Immunol. 2012; 33:168–173. [PubMed: 22342741]
5. Buck MD, O'Sullivan D, Pearce EL. T cell metabolism drives immunity. J Exp. Med. 2015; 212:1345–1360. [PubMed: 26261266]
6. Cham CM, Driessens G, O'Keefe JP, Gajewski TF. Glucose deprivation inhibits multiple key gene expression events and effector functions in CD8+ T cells. Eur. J Immunol. 2008; 38:2438–2450. [PubMed: 18792400]
7. Cham CM, Gajewski TF. Glucose availability regulates IFN-gamma production and p70S6 kinase activation in CD8+ effector T cells. J Immunol. 2005; 174:4670–4677. [PubMed: 15814691]
8. Wang R, Green DR. Metabolic reprogramming and metabolic dependency in T cells. Immunol. Rev. 2012; 249:14–26. [PubMed: 22889212]
9. He S, Kato K, Jiang J, Wahl DR, Mineishi S, Fisher EM, Murasko DM, Glick GD, Zhang Y. Characterization of the metabolic phenotype of rapamycin-treated CD8+ T cells with augmented ability to generate long-lasting memory cells. PloS one. 2011; 6:e20107. [PubMed: 21611151]
10. Powell JD, Delgoffe GM. The Mammalian Target of Rapamycin: Linking T Cell Differentiation, Function, and Metabolism. Immunity. 2010; 33:301–311. [PubMed: 20870173]
11. Wang R, Dillon CP, Shi L, Milasta S, Carter R, Finkelstein D, McCormick LL, Fitzgerald P, Chi H, Munger J, Green DR. The Transcription Factor Myc Controls Metabolic Reprogramming upon T Lymphocyte Activation. Immunity. 2011; 35:871–882. [PubMed: 22195744]
12. Araki K, Turner AP, Shaffer V, Gangappa S, Keller SA, Bachmann MF, Larsen CP, Ahmed R. mTOR regulates memory CD8 T-cell differentiation. Nature. 2009; 460:108–112. [PubMed: 19543266]
13. Nam J. Rapamycin: could it enhance vaccine efficacy? Expert Rev. Vaccines. 2009; 8:1535–1539. [PubMed: 19863245]
14. Snow AL, Pandiyan P, Zheng L, Krummey SM, Lenardo MJ. The power and the promise of restimulation-induced cell death in human immune diseases. Immunol. Rev. 2010; 236:68–82. [PubMed: 20636809]
15. Lenardo MJ. Interleukin-2 programs mouse alpha beta T lymphocytes for apoptosis. Nature. 1991; 353:858–861. [PubMed: 1944559]
16. Russell JH, White CL, Loh DY, Meleedy-Rey P. Receptor-stimulated death pathway is opened by antigen in mature T cells. Proc. Natl. Acad. Sci. U.S.A. 1991; 88:2151–2155. [PubMed: 1826050]
17. Ruffo E, Malacarne V, Larsen SE, Das R, Patrussi L, Wülfing C, Biskup C, Kapnick SM, Verbist K, Tedrick P, Schwartzberg PL, Baldari CT, Rubio I, Nichols KE, Snow AL, Baldanzi G, Graziani A. Inhibition of diacylglycerol kinase α restores restimulation-induced cell death and reduces immunopathology in XLP-1. SCi. Transl. Med. 2016; 8:321–327.
18. Snow AL, Marsh RA, Krummey SM, Roehrs P, Young LR, Zhang K, van Hoff J, Dhar D, Nichols KE, Filipovich AH, Su HC, Bleesing JJ, Lenardo MJ. Restimulation-induced apoptosis of T cells is impaired in patients with X-linked lymphoproliferative disease caused by SAP deficiency. J Clin Invest. 2009; 119:2976–2989. [PubMed: 19759517]
19. Ashwell JD, Cunningham RE, Noguchi PD, Hernandez D. Cell growth cycle block of T cell hybridomas upon activation with antigen. J Exp. Med. 1987; 165:173–194. [PubMed: 3491868]
20. Green DR, Droin N, Pinkoski M. Activation-induced cell death in T cells. Immunol. Rev. 2003; 193:70–81. [PubMed: 12752672]
21. Budd RC. Activation-induced cell death. Curr. Opin. Immunol. 2001; 13:356–362. [PubMed: 11406369]
22. Katz G, L. Snow A, Lenardo MJ. Fluuorescence-activated cell sorting-based quantitation of T cell receptor restimulation-induced cell death in activated, primary human T cells. Methods in Molecular Biology. 2013; 979:15–23. [PubMed: 23397384]
23. Drury G, Di Marco S, Dormoy-Raclet V, Desbarats J, Gallouzi I. FasL Expression in Activated T Lymphocytes Involves HuR-mediated Stabilization. J Biol Chem. 2010; 285:31130–31138. [PubMed: 20675370]
24. Chang CH, Curtis JD, Maggi LB Jr. Faubert B, Villarino AV, O'Sullivan D, Huang SC, van der Windt GJ, Blagih J, Qiu J, Weber JD, Pearce EJ, Jones RG, Pearce EL. Posttranscriptional control of T cell effector function by aerobic glycolysis. Cell. 2013; 153:1239–1251. [PubMed: 23746840]

25. Donnelly RP, Finlay DK. Glucose, glycolysis and lymphocyte responses. Mol Immunol. 2015; 68:513–519. [PubMed: 26260211]
26. Boehme SA, Lenardo MJ. Propriocidal apoptosis of mature T lymphocytes occurs at S phase of the cell cycle. Eur J Immunol. 1993; 23:1552–1560. [PubMed: 8325332]
27. Wesselborg S, Kabelitz D. Activation-driven death of human T cell clones: time course kinetics of the induction of cell shrinkage, DNA fragmentation, and cell death. Cell Immunol. 1993; 15:234–241.
28. Yang L, Kotomura N, K. Ho Y, Zhi H, Bixler S, Schell MJ, Giam CZ. Complex cell cycle abnormalities caused by human T-lymphotropic virus type 1 Tax. J Virol. 2011; 85:3001–3009. [PubMed: 21209109]
29. Refaeli Y, Van Parijs L, Alexander SI, Abbas AK. Interferon γ Is Required for Activation-induced Death of T Lymphocytes. J Exp Med. 2002; 196:999–1005. [PubMed: 12370261]
30. Kataoka T, Shinohara N, Takayama H, Takaku K, Kondo S, Yonehara S, Nagai K. Concanamycin A, a powerful tool for characterization and estimation of contribution of perforin- and Fas-based lytic pathways in cell-mediated cytotoxicity. J Immunol. 1996; 156:3678–3686. [PubMed: 8621902]
31. Pollizzi KN, Powell JD. Integrating canonical and metabolic signalling programmes in the regulation of T cell responses. Nat Rev Immunol. 2014; 14:435–446. [PubMed: 24962260]
32. Delmore JE, Issa GC, Lemieux ME, Rahl PB, Shi J, Jacobs HM, Kastritis E, Gilpatrick T, Paranal RM, Qi J, Chesi M, Schinzel AC, McKeown MR, Heffernan TP, Vakoc CR, Bergsagel PL, Ghobrial IM, Richardson PG, Young RA, Hahn WC, Anderson KC, Kung AL, Bradner JE, Mitsiades CS. BET bromodomain inhibition as a therapeutic strategy to target c-Myc. Cell. 2011; 146:904–917. [PubMed: 21889194]
33. Kavurma MM, Khachigian LM. Signaling and transcriptional control of Fas ligand gene expression. Cell Death Differ. 2003; 10:36–44. [PubMed: 12655294]
34. Brunner T, Kasibhatla S, Pinkoski MJ, Frutschi C, Yoo NJ, Echeverri F, Mahboubi A, Green DR. Expression of Fas ligand in activated T cells is regulated by c-Myc. J Biol Chem. 2000; 275:9767–9772. [PubMed: 10734130]
35. Sriram G, Martinez JA, McCabe ERB, Liao JC, Dipple KM. Single-Gene Disorders: What Role Could Moonlighting Enzymes Play? Am. J Hum. Genet. 2005; 76:911–924. [PubMed: 15877277]
36. Xu X, Araki K, Li S, Han J-H, Ye L, Tan WG, Konieczny BT, Bruinsma MW, Martinez J, Pearce EL, Green DR, Jones DP, Virgin HW, Ahmed R. Autophagy is essential for effector CD8+ T cell survival and memory formation. Nat Immunol. 2014; 15:1152–1161. [PubMed: 25362489]
37. Joshi NS, Cui W, Chandele A, Lee HK, Urso DR, Hagman J, Gapin L, Kaech SM. Inflammation directs memory precursor and short-lived effector CD8(+) T cell fates via the graded expression of T-bet transcription factor. Immunity. 2007; 27:281–295. [PubMed: 17723218]
38. Amsen D, Backer RA, Helbig C. Decisions on the road to memory. Adv Exp Med Biol. 2013; 785:107–120. [PubMed: 23456843]
39. Marks-Konczalik J, Dubois S, Losi JM, Sabzervari H, Yamada N, Feigenbaum L, Waldmann T, Tagaya Y. IL-2-induced activation-induced cell death is inhibited in IL-15 transgenic mice. Proc. Natl. Acad. Sci. U.S.A. 2000; 97:11445–11450. [PubMed: 11016962]
40. Yajima T, Yoshihara K, Nakazato K, Kumabe S, Koyasu S, Sad S, Shen H, Kuwano H, Yoshikai Y. IL-15 regulates CD8+ T cell contraction during primary infection. J Immunol. 2006; 176:507–515. [PubMed: 16365444]
41. Rao RR, Li Q, Odunsi K, Shrikant PA. The mTOR kinase determines effector versus memory CD8+ T cell fate by regulating the expression of transcription factors T-bet and Eomesodermin. Immunity. 2010; 32:67–78. [PubMed: 20060330]

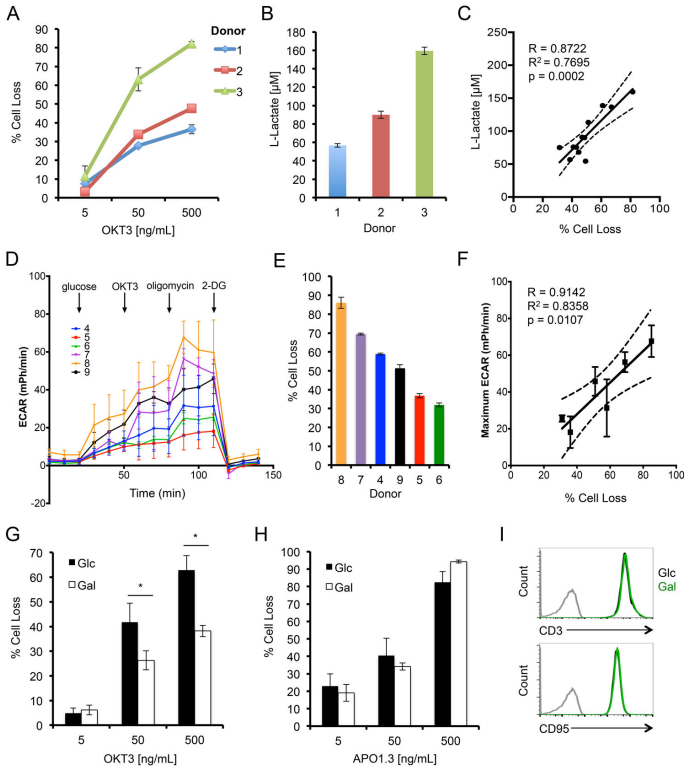

Figure 1. Increased RICD sensitivity in glycolytic CD8$^+$ T cells

(A) Activated T cells from 3 normal donors (1-3) were restimulated with OKT3 Ab. Percent cell loss was measured 24 hrs later by PI staining and flow cytometry. **(B)** L-Lactate was measured in T cell supernatants by ELISA after 4 hrs of OKT3 restimulation. **(C)** Linear regression analysis comparing maximum % cell loss versus L-lactate production for 12 independent donors, including 95% confidence interval (dashed line). Pearson correlation R=0.8722, R^2=0.7695 and p=0.0002. **(D)** Seahorse analysis of extracellular acidification rate (ECAR) of 6 different donors (4-9). **(E)** RICD sensitivity of the same 6 donors (4-9) used for Seahorse analysis **(F)** Linear regression analysis comparing maximum % cell loss versus maximum ECAR for 6 independent donors, including 95% confidence interval (dashed line). Pearson correlation R=0.9142, R^2=0.8358 and p=0.0107. **(G)** Activated T cells cultured in glucose (Glc) or galactose (Gal)-containing media for ~14 days were restimulated and analyzed as in (A). Data represent % cell loss (avg ± SEM) for 5 individual donors for a 24h RICD assay. Glc and Gal T cells were compared by two-way ANOVA: OKT3 [5] n.s, [50] p=0.0057, [500] p=0.0003. **(H)** Activated T cells as in (G) were stimulated with anti-FAS agonistic Ab APO1.3 for 24 hrs. Data represent % cell loss (avg ± SEM) for 3 individual donors. Two-way ANOVA analysis showed no significant differences. **(I)** Representative FACS surface staining of CD3 (upper panel) and CD95 (lower panel) between Glc (black) and Gal (green) T cells versus isotype control (grey).

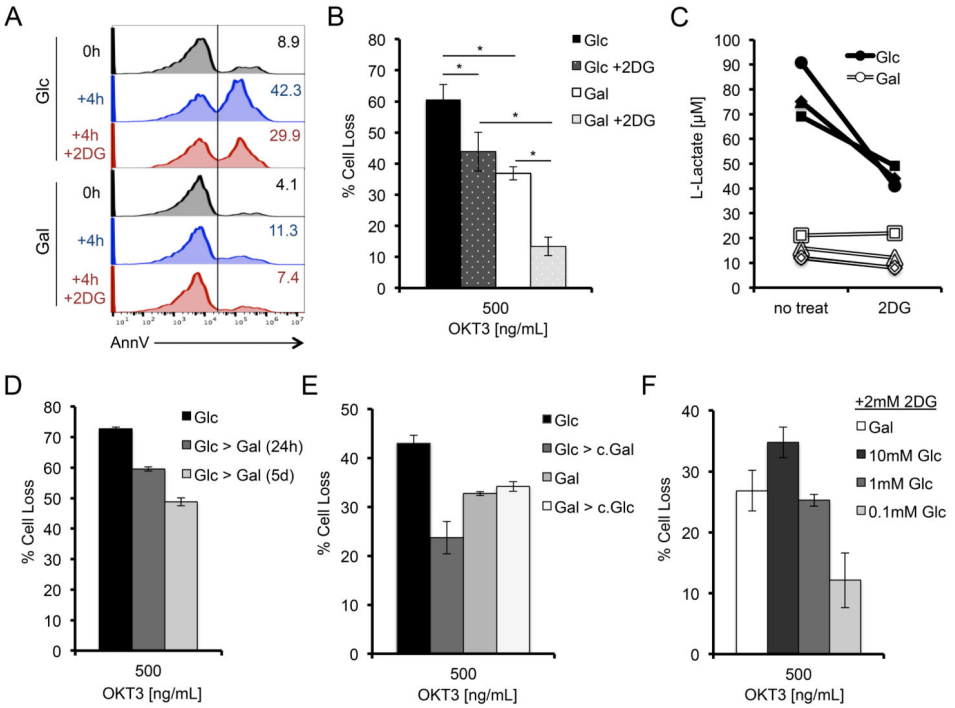

Figure 2. Acute glucose availability governs RICD sensitivity

(A) Annexin V binding to Glc or Gal T cells at baseline, or after 4 hr OKT3 restimulation ± 2-DG (2 mM) analyzed by flow cytometry. Numbers denote % of AnnexinV$^+$ T cells. **(B)** Glc or Gal T cells were restimulated with 500 ng/ml OKT3 for 24 hrs ± 2 mM 2-DG pre-treatment, and analyzed for RICD as in Fig 1D. Data represent % cell loss (avg ± SEM) for 6 individual donors. Treatments were compared by two-way ANOVA: Glc-Gal $p<0.0001$, Glc-Glc+2-DG $p=0.0003$, Glc+2DG-Gal+2-DG $p<0.0001$, Gal-Gal+2DG $p<0.0001$. **(C)** L-Lactate was measured in T cell supernatants after 4 hours of OKT3 restimulation ± 2-DG, data represents 4 individual donors. Lines connect data points for each single donor. **(D)** Glc T cells were maintained or switched into Gal media on day 9 or day 13 in culture, then assayed for RICD sensitivity on day 14 as in (B). Data (average ± SD of technical replicates) are representative of 3 independent experiments using different donors. **(E)** Glc or Gal T cells were placed into fresh media or swapped into 3 day conditioned media of the opposite sugar with added IL-2 and analyzed for RICD sensitivity. Data (average ± SD of technical replicates) are representative of 3 independent experiments using different donors. **(F)** Gal T cells were washed and resuspended in media containing titrating doses of glucose (0.1 – 10 mM) and tested for RICD sensitivity as in (B) + 2-DG treatment. Data (avg ± SD of technical replicates) are representative of 3 independent experiments using different donors.

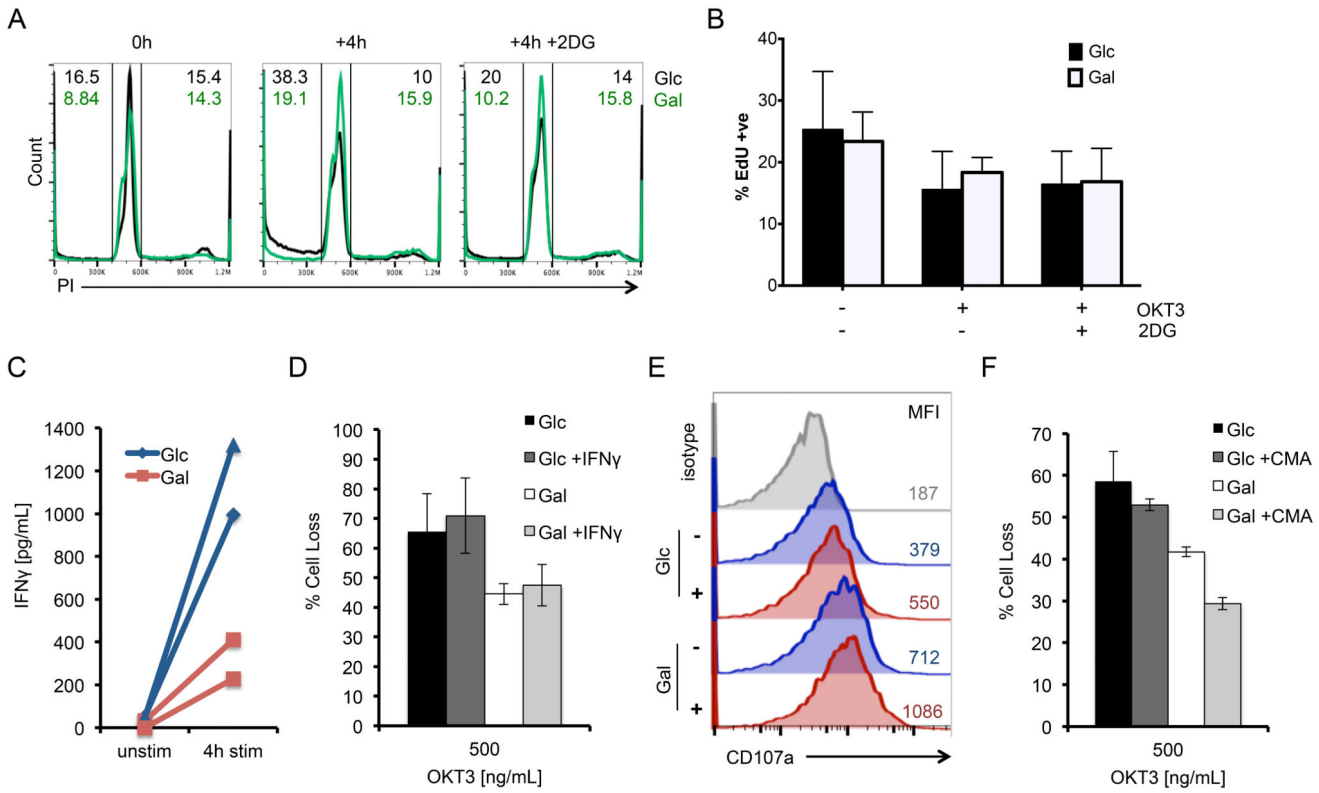

Figure 3. Cell cycle progression and differential effector function do not contribute to differential RICD sensitivity in Glc vs. Gal T cells

(A) Flow cytometric PI cell cycle analysis of Glc (black) and Gal T cells (green) at baseline and after 4 hours of OKT3 restimulation ± 2-DG. Numbers denote % cells in sub-G1/ apoptotic gate (upper left) or S+G2/M (upper right). Data are representative of 3 independent experiments using different donors. **(B)** EdU incorporation by Glc and Gal T cells treated as in (A) was measured by flow cytometry. Data (average ±SD) represent 4 independent experiments using different donors. Conditions compared by T-test were all n.s. **(C)** Secreted IFNγ was measured in Glc (blue) vs. Gal T cell (red) supernatants by ELISA after 4 hours of OKT3 restimulation; n=2 donors. Lines connect data points for each single donor. **(D)** Glc and Gal T cells were pretreated with 10 ng/mL IFNγ for 30 minutes, then assayed for RICD as above. Data represent % cell loss (avg ±SEM) of 3 donors. Treatments were compared by two-way ANOVA: (D) Glc-Gal p=0.0176, Glc+IFN-γ-Gal+IFN-γ p= 0.0140, Glc-Glc+IFN-γ n.s, Gal-Gal+IFN-γ n.s. **(E)** Representative surface staining and MFI of CD107a between Glc (upper) and Gal (lower) T cells versus isotype control (grey) at baseline (blue) or after 4 hours of restimulation (red) by flow cytometry. **(F)** Glc and Gal T cells were pretreated with 5μg/mL concanamycin A (CMA) for 30 minutes, then assayed for RICD as above. Data represent % cell loss (avg ±SEM) of 3 donors. Treatments were compared by two-way ANOVA: Glc-Gal p=0.0366, Glc+CMA-Gal+CMA p=0.0223, Glc-Glc+CMA n.s, Gal-Gal+CMA n.s.

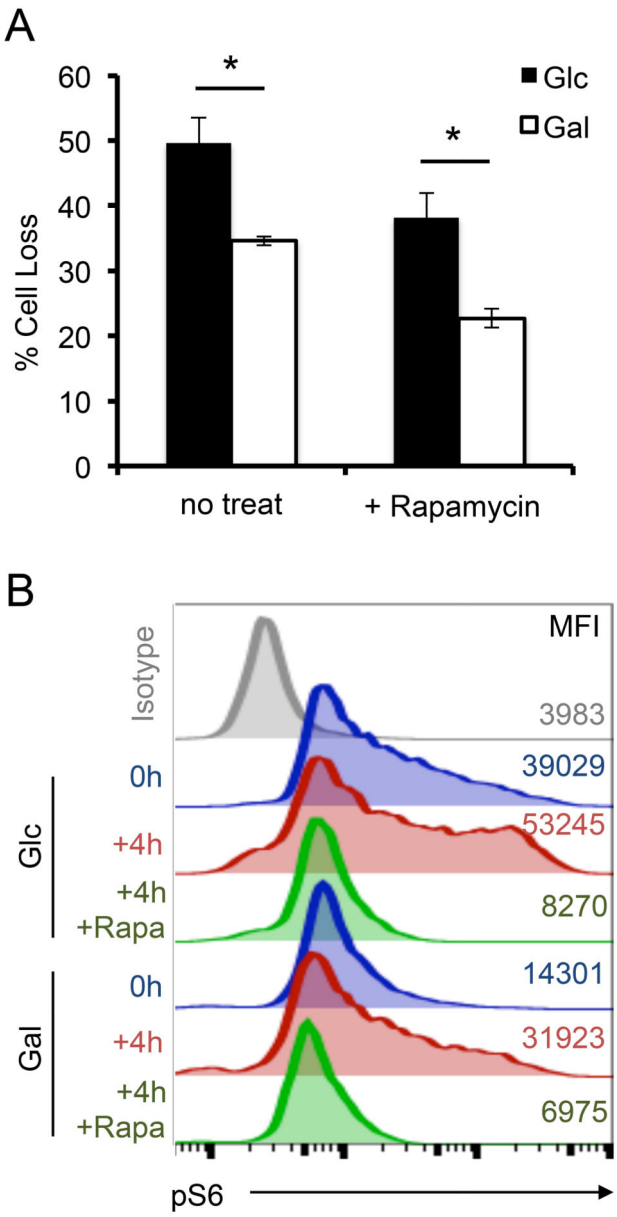

Figure 4. Differential RICD is independent of mTORC1 activity

(A) Glc or Gal T cells were restimulated ± 2.7 μM rapamycin pre-treatment, and analyzed for RICD as previously described. Data represent % cell loss (avg ± SEM) for 4 individual donors. Data were compared by T-test: Glc-Gal p=0.0185, Glc+Rapa-Gal+Rapa p=0.01864. **(B)** Intracellular staining for pS6 in Glc or Gal T cells at baseline, or after 4 hr OKT3 restimulation ± 2mM 2-DG or ± 2.7 μM rapamycin analyzed by flow cytometry. Numbers denote MFI. Data are representative of 3 independent experiments using different donors.

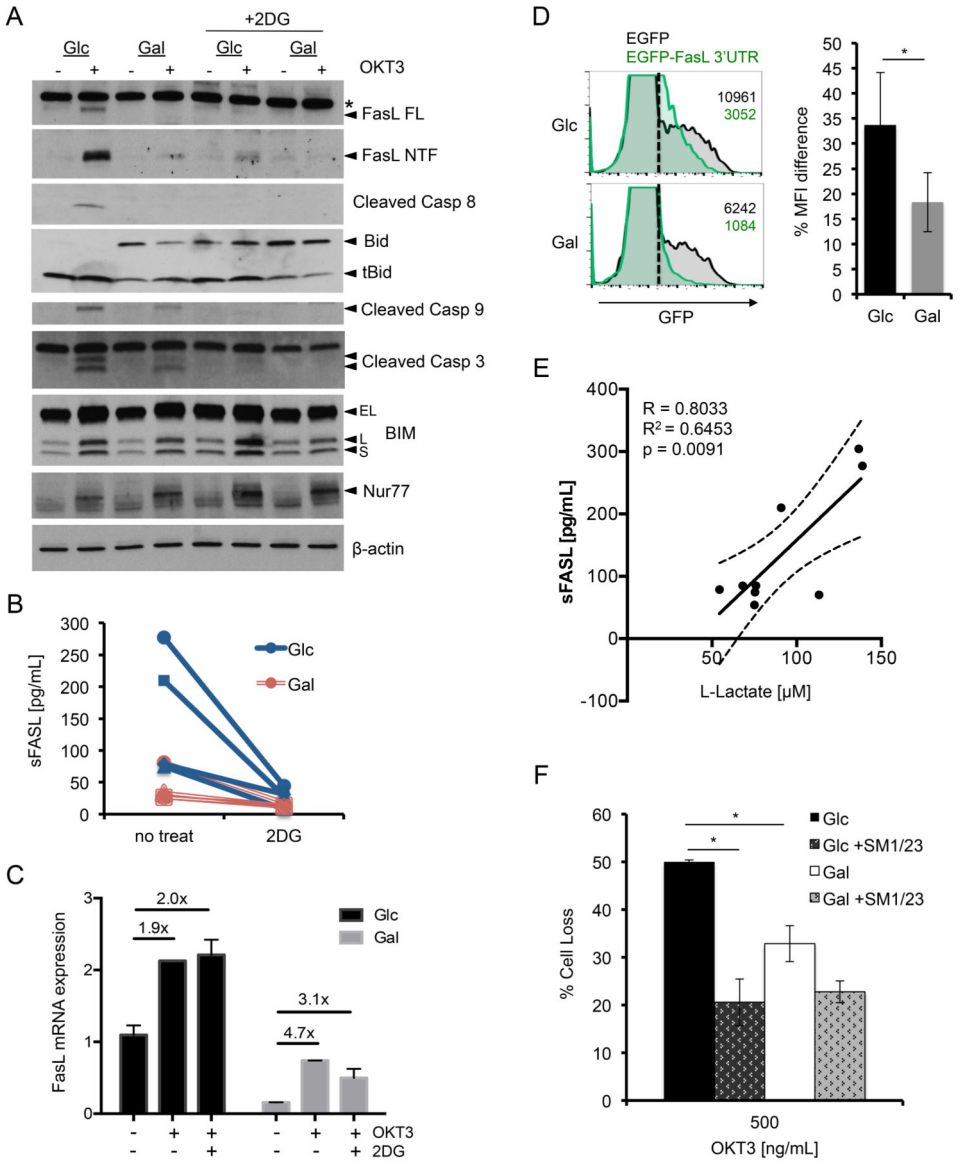

Figure 5. Glycolysis enhances RICD specifically by facilitating FASL induction after TCR restimulation

(A) Lysates of Glc and Gal T cells at baseline or after 4 hr OKT3 restimulation ± 2-DG treatment were separated by SDS-PAGE and immunoblotted for the indicated proteins. Asterisk denotes non-specific band; arrows denote specific bands. β-actin serves as a loading control. Data are representative of 3 independent experiments using different donors. **(B)** Soluble FASL (sFASL) was measured in Glc (blue) vs. Gal T cell (red) supernatants by ELISA after 4 hours of OKT3 restimulation ± 2-DG, n=4 donors. Lines connect data points for each single donor. **(C)** Relative expression of FASL message measured by qPCR of Glc and Gal T cells treated as in (A). FASL mRNA was standardized to RPL13 control for each sample; Glc baseline was normalized to 1. Data (average ± SD of technical replicates) are representative of 2 independent experiments using different donors. Values in figure represent fold change from unstimulated sample. **(D)** Glc and Gal T cells were transfected

with a FASL 3' UTR GFP reporter plasmid (green histograms) or control GFP plasmid (black histograms), and analyzed for GFP expression after 6 hours by flow cytometry. Representative histograms are shown at left, including MFI values for the GFP^+ population (right of dotted line). Bar graph represents avg ±SD of % change in MFI (3'UTR-GFP/GFP alone) for 3 independent donors. **(E)** Linear regression analysis comparing sFASL and L-lactate production in restimulated Glc T cell supernatants for 9 independent donors, including 95% confidence interval (dashed line). Pearson correlation R= 0.8033, R^2= 0.6453, p=0.0091. **(F)** Glc and Gal T cells were pretreated with anti-FAS blocking Ab SM1/23 for 30 min, then assayed for RICD as above. Data represent % cell loss (avg ±SEM) for 3 independent donors. Treatments were compared by two-way ANOVA: Glc-Gal p=0.0124, Glc-Glc+SM1/23 p=0.0005, Glc+SM1/23-Gal+SM1/23 n.s, Gal-Gal+SM1/23 n.s.